JOURNAL OF Applied Polymer SCIENCE

Synthesis, characterization, catalytic and splinting activity of nano Ag end capped L-glutathione bridged amphiphilic diblock copolymer

Muthuramalingam Jeyapriya, Balakrishnan Meenarathi, Ramasamy Anbarasan
Department of Polymer Technology, Kamaraj College of Engineering and Technology, Virudhunagar, Tamilnadu 626001, India
Correspondence to: R. Anbarasan (E-mail: anbu_may3@yahoo.co.in)

ABSTRACT: L-glutathione, a naturally occurring environmental friendly amino acid, was used as an initiator towards the ring opening polymerization (ROP) of ε-caprolactone (CL) followed by the ROP of tetrahydrofuran (THF). The thiol group of L-glutathione reduces Ag^+ ions and chemically bound to the surface of Ag nanoparticles. The ROP of CL was carried out at 160 °C under nitrogen atmosphere in the presence of stannous octoate(SO) as catalyst whereas the ROP of THF was carried out at 45 °C for 24 h in the presence of phthalic anhydride (PAH) as a comonomer. The synthesized homo, di and nano Ag end capped diblock copolymers were characterized by FTIR, DSC, TGA, FESEM, high resolution transmission electron microscope (HRTEM), EDAX, GPC, nuclear magnetic resonance (NMR), Fluorescence and CD. Further the application of diblock copolymer was tested for splinting activity. The catalytic reduction of 4-nitrophenol (NP) in the presence of nano Ag end capped diblock copolymer was carried out with the assistance of sodium borohydride as a reducing agent and the apparent rate constant (k_{app}) was determined and compared with the literature values. © 2016 Wiley Periodicals, Inc. J. Appl. Polym. Sci. **2016**, *133*, 43804.

KEYWORDS: catalysts; differential scanning calorimetry; ring opening polymerization; spectroscopy

Received 21 December 2015; accepted 17 April 2016
DOI: 10.1002/app.43804

INTRODUCTION

Biodegradable and biocompatible synthetic polymers have tempted the polymer scientist for the past two decades because of their applications in various science and engineering fields particularly, as a drug delivery material, known as biomedical polymers. There are lots of bio-medical synthetic polymers available in the market even then PCL is given much more importance due to its eco-friendly nature and less cytotoxic effects.[1] Recently, the application of PCL is extended to splinting activity.[2] Generally, the PCL is synthesized through ring-opening polymerization (ROP) of CL in a bulk polymerization method.[3–6] In order to increase the physical, chemical and biomedical applications of PCL, it was copolymerized with other monomers.[7,8] Copolymerization of CL and benzyloxymethylglycolide was done.[9] The resultant copolymer exhibited enhanced hydrophilicity, increased degradation rate and improved cell material interaction. The PCL based multiblock copolymer was synthesized with chain extender process.[10] Zhao *et al.* [11] reported about the PCL based multiblock copolymers with improved enzymatic bio-degradation. In 2010, Cuong and research team synthesized PCL based triblock copolymer and used as a drug carrier.[12] No reports are available based on the preparation of PCL based diblock copolymer using a biomaterial like glutathione as a bridging agent. In the present investigation glutathione, an amino acid is used as a bridging agent for the preparation of a diblock copolymer consists of PCL and poly (tetrahydrofuran) (PTHF) for the first time, towards the bio-medical application and catalytic field.

Homo and block copolymer of THF offers quite a number of valuable properties and bio-medical applications.[2,13–18] Guo and coworkers[19] synthesized the PTHF via cationic ROP mechanism. In 2012, Bouchama *et al.*[20] reported about the copolymer of CL and THF. Sari *et al* [3] synthesized a copolymer made of THF and styrene monomer.[21] Copolymer made of epichlorohydrin (ECH) and THF was reported in the literature.[22] It was found that THF was grafted onto the copolymer backbone.[23] THF was copolymerized with monomer or polymer like PEG,[24] oxetane,[25] PEO,[26] PAH[27] and methyl methacrylate.[28] Only few reports are available regarding the block copolymerization of THF with PCL. It also indicates that for the preparation of diblock copolymer an amino acid like glutathione was not used as an initiator. This urged us to do the present investigation.

Glutathione is a reactive chiral bio-material with two carboxyl groups, one amino group, one thiol group and two amide

Additional Supporting Information may be found in the online version of this article.

linkages. Due to the presence of thiol group, it acts as a reducing agent.[29] Glutathione is a major endogenic antioxidant material produced by the cells which is used in the metabolic and biochemical reactions. The amino acids are basic units of proteins that have luminescence property. Recently, biochemists turned their attention towards the helical and β-sheet structure analysis of glutathione [30–32] because of their biological importance. The coordination chemistry on α-amino acids complexes are explained in the literature by Hakimi *et al.*[33] The application of such a biologically interesting compound is very few. By keeping this key point, the present investigation was designed, i.e., glutathione was used as an initiator toward the ROP of CL and THF. This is the novelty of the present investigation.

The physical, chemical and surface catalytic activity of metal nanoparticles depends on the size and shape of metal nanoparticles. Among the various metal nanoparticles, Ag nanoparticle played a vital role because of its antimicrobial activity, ease of synthesis and economically cheaper one.[34] In 2014, Hsu *et al.*[35] reported about the catalytic effect of Ag reduced graphene amide nanoparticle towards the reduction of NP. The catalytic activity of Ag nanoparticle toward the reduction of NP was proved by different research teams.[36–39] The nanosized Ag has an ability to catalyze the reduction of 4-nitrophenol to 4-aminophenol. Also, in all those studies the Ag nanoparticles simply be dispersed or encapsulated by the polymer chains. But in the present investigation, apart from encapsulation, the Ag nanoparticle is chemically conjugated with the sulfur atom of glutathione. Moreover, these types of amphiphilic polymers are not having any side reactions. Above all, after the reduction reaction the catalyst can be easily isolated by the addition of diethyl ether, as a solid catalyst.

EXPERIMENTAL

Materials

Tetrahydrofuran (THF), chloroform ($CHCl_3$), phthalic anhydride (PAH), and diethylether were purchased from S.D. Fine chemicals, India. Stannous octoate (SO, Merck, India) and L-glutathione (Ottochemi, India) were purchased and used as it was received. ϵ-caprolactone (CL) was purchased from Aldrich, India. $AgNO_3$ was received from CDH, India. PET fabric was received as a gift sample from Rajapalayam, India. Double distilled (DD) water was used for solution making purpose.

Synthesis of nano Ag end capped PC L-glutathione-PTHF diblock copolymer includes three steps.

Step-I Synthesis of PCL (P1)

The ROP of CL was carried out by bulk polymerization method. The procedure is described in brief. 2 g CL monomer was taken in a 25 mL capacity round bottomed flask (RBF). The SO, catalyst was charged into the RBF. The monomer to catalyst (M/C) ratio was maintained at 1000. This will help to increase the molecular weight of the polymer without any branching or cross linking. Also reduces the backbiting reaction. Required amount of L-glutathione, initiator (M/I = 100) was added and the RBF was purged with sulfur free nitrogen gas under mild stirring at room temperature for 10 min. Then, the sealed RBF was put into an oil bath at 160 °C for 2 h. At higher temperature only the ROP of CL is favorable one with moderate molecular weight. During the course of the reaction, the medium become highly viscous. L-glutathione contains different functional groups like amine, thiol and carboxyl groups, among them the amino group might involved in the ROP of CL. At the end of the reaction, the RBF was removed from the oil bath, cooled and the contents were dissolved in 25 mL $CHCl_3$ and transferred to the 500 mL beaker. The PCL was re-precipitated by the addition of 250 mL diethyl ether.[40] Thus obtained white precipitate was washed three times with DD water to remove the unreacted monomer, L-glutathione and SO. After washing thoroughly, the white precipitate thus obtained was freeze dried. The purified PCL sample was weighed and stored in a zip lock cover. The product is L-glutathione end capped PCL (P1). The reaction is mentioned in Scheme 1. The yield was calculated as 99% (Table I).

Step-II Synthesis of PCL-L-Glutathione-PTHF Diblock Copolymer (P2)

The synthesis procedure for the PCL-glutathione-PTHF diblock copolymer is given in brief: 0.50 g of PCL obtained in the step-I was considered as a macro initiator. 20 mL of THF (as a co-monomer) was charged in a 50 mL RBF. 0.01 g PAH and 0.50 g macro initiator (PCL) were added to the reaction mixture and heated to 45 °C under nitrogen purging with stirring. The PAH induced the ROP of THF. The carboxyl group present in the L-glutathione might involve in the ROP of PAH and THF.[2] After 24 h of ROP, the contents were poured into the 100 mL dil. HCl solution to arrest the ROP of THF. At the end of the reaction, the contents were evaporated to dryness and 100 mL of DD water was added, stirred well, and dried by freeze drying method. After drying one can get a pale brown colored PCL-L-glutathione-PTHF diblock copolymer. Thus obtained polymer sample (P2) was weighed and stored under N_2 atmosphere. The yield was determined as 85% (Table I). The reaction is mentioned in Scheme 1.

Step-III Synthesis of Nano Ag End Capped PCL-L-Glutathione-PTHF Diblock Copolymer (P3)

In the third step, 1.0 g of L-glutathione bridged diblock copolymer was dissolved in 25 mL of THF taken in a 100 mL RBF fitted with a condenser. 0.50 g $AgNO_3$ was dissolved in 10 mL of DD water and mixed with the diblock copolymer solution. The contents were heated to 40 °C for 2 h by the ice-cold water circulation in the condenser. In such a way one can avoid the evaporation of THF solvent. During the mixing, a brown color precipitate appeared.[41] At the end of the reaction, the contents were dried by freeze drying method. Finally, one can get a brown colored nano Ag end capped PCL-L-glutathione-PTHF diblock copolymer. During the reaction, the Ag^+ was reduced[42] to Ag^0. This was done through the polyol methodology. Sometimes the thiol or amino group present in the L-glutathione initiator might involve in the reduction reaction. The reaction is mentioned in Scheme 1. The yield was calculated as 76% (Table I). This low yield is due to the following reasons. (i) removal of HNO_3 as a by-product and (ii) dissolution of samples in THF solvent.

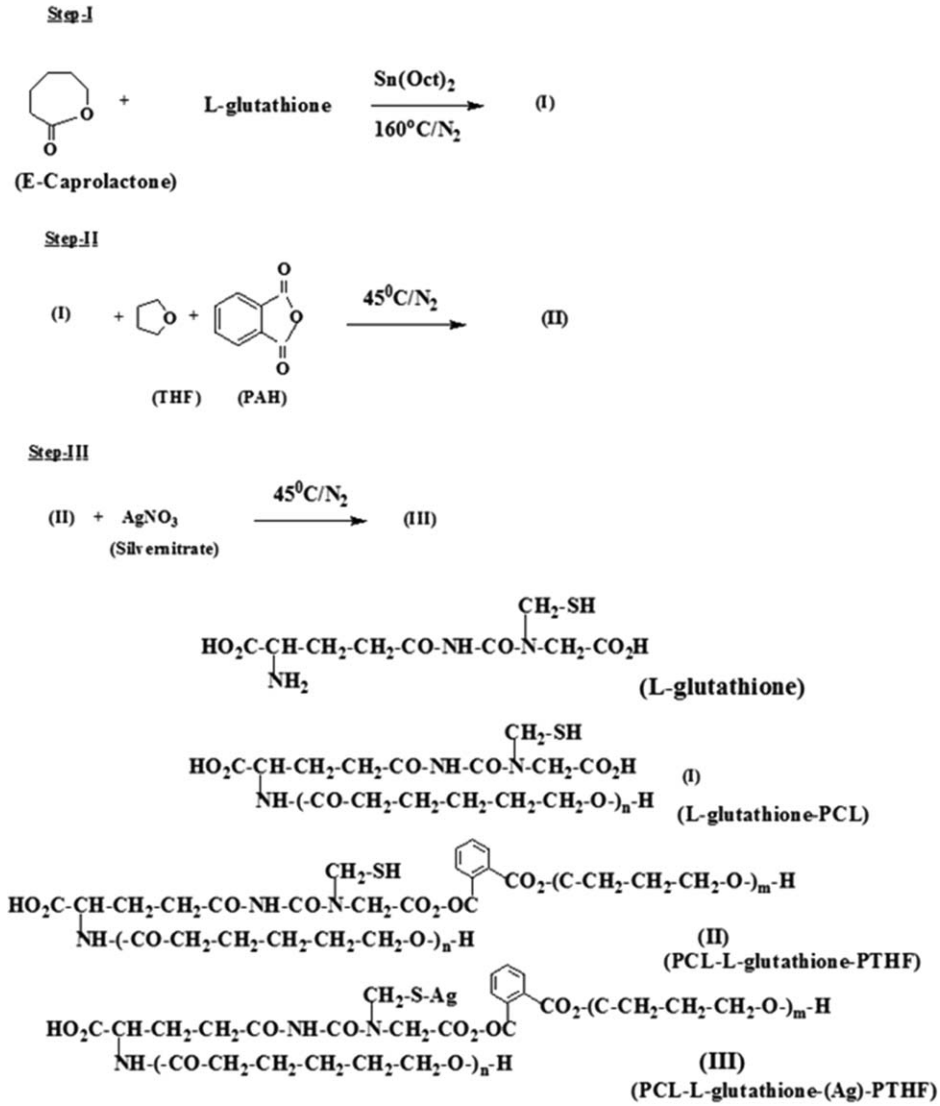

Scheme 1. Synthesis of nano Ag end capped diblock copolymer.

Wound Healing Activity

The splinting activity of the synthesized polymeric systems is expressed in terms of high mechanical and solvent absorption properties. It is necessary to find out the mechanical properties particularly tensile strength and elongation with the solvent absorption properties. The raw fabrics of 10 cm length and 5 cm breadth are taken and weighed. 1 g of polymer (P1 or P2 or P3) was dissolved in 50 mL of chloroform solvent. The raw fabric was immersed in the polymer solution under constant stirring for 5 h for coating. After the coating, the fabric was dried and weighed. It gives the weight of the polymer coated over the fabric material. For each polymer coating, two raw fabrics are taken and the weight is calculated for the average values. The polymer coated fabric of P1, P2 and P3 is taken and weighed. Each weighed samples is immersed in water under stirring for 5 min. After that, the fabric is taken immediately and weighed in wet condition. The difference between the dry fabric and the wet fabric gives the net water absorption values for the polymer coated fabric material. The chloroform absorption is studied for the P1, P2, and P3 polymer coated fabrics by the above method. The polymer coated fabrics was taken and weighed. Each weighed samples was immersed in chloroform under stirring for 5 mins. After that, the fabric is taken immediately and weighted in wet condition. The difference between the dry fabric and the wet fabric gives the net chloroform absorption values for the polymer coated fabric material.

Catalytic Reduction Study

Nitrophenol of 0.0067 g is dissolved in the aqueous medium of 50 mL (1×10^{-3}M). 0.02 g of P3 sample is dissolved in the

Table I. % Yield and GPC Data of Polymer Systems

System	% Yield	M_w (g/mol)	M_n	P.D
P1	99	3415	2119	1.61
P2	85	3660	2056	1.78
P3	76	3868	2137	1.81

20 mL of water separately. Mixture of 2 mL of nitrophenol solution and 1 mL of P3 solution is taken with 0.02 g of sodium borohydride, a reducing agent. The UV-visible spectrum was taken and marked as initial absorbance (A_o). For constant time interval the absorbance (A) were recorded until the peak of nitrophenol at 400 nm disappears. The apparent rate constant was calculated from the slope of $\ln(A/A_0)$ Vs time graph.

Characterizations

Fourier transform infrared (FTIR) spectra for the samples were recorded with the help of a Shimadzu 8400 S, Japan instrument by the KBr pelletization method from 400 to 4000 cm^{-1}. The FTIR disc was prepared under 7 tons of pressure. Fluorescence emission spectral measurement was carried out with the help of an instrument Elico SL 172, India. Circular dichroism (CD) was studied using Jasco J-715 model instrument. The surface morphology and particle sizes of the grafted samples were determined by Field emission scanning electron microscope (FESEM) method using Hitachi S4800 Japan model instrument. Differential scanning calorimetry (DSC) and thermo gravimetric analysis (TGA) were measured using Universal V4.4A TA Instruments under nitrogen atmosphere at the heating rate of 10 °C min^{-1} from room temperature to 600 °C. The second heating scan of the sample was considered to delete the previous thermal history of the sample. The molecular weight determination of diblock copolymer samples was carried out using gel permeation chromatography, Perkin Elmer Series 200 in THF solvent and poly (styrene) as an internal standard. ^1H and ^{13}C-nuclear magnetic resonance (NMR) (500 MHz) spectra were obtained using an NMR apparatus (Varian, Unity Inova-500 NMR) at room temperature in $CDCl_3$ solvent. High resolution transmission electron microscope (HRTEM) measurements for P1, P2, and P3 samples were carried out using JEM-200 CX, USA transmission electron microscope instrument. Tensile Strength was measured using the instrument Universal Tensile Tester, Deepak Polyplast, India.

RESULTS AND DISCUSSION

The functionalities present in the polymer systems were confirmed by FTIR spectroscopic technique. Figure 1(a) indicates the FTIR spectrum of L-glutathione end capped PCL. The —NH, —OH, C—H symmetry and anti-symmetry stretching were noticed at 3439, 3373, 2864, and 2947 cm^{-1} respectively. The carbonyl stretching and C—O—C linkage can be seen at 1729 and 1187 cm^{-1}, respectively. The C=O and C—O—C stretching result is matched with the earlier publication.[43] The C—N stretching of L-glutathione appeared at 1370 cm^{-1}.[44] The C═H out of plane bending vibration (OPBV) appeared at 728 cm^{-1}. Figure 1(b) indicates the FTIR spectrum of PCL-PTHF diblock copolymer, here also one can see the above said peaks corresponding to PCL. Some new peaks also appeared corresponding to PTHF segments. During the copolymerization, PAH was used as a comonomer. The aromatic C—H symmetry and antisymmetry stretching appeared at 2521 and 2652 cm^{-1} respectively. The carbonyl stretching is appeared as a doublet peak due to the aliphatic PCL chains and aromatic PAH chains. The aromatic C═O stretching appeared at 1668 cm^{-1}, whereas the aliphatic C═O stretching of PCL appeared at 1719 cm^{-1}. A

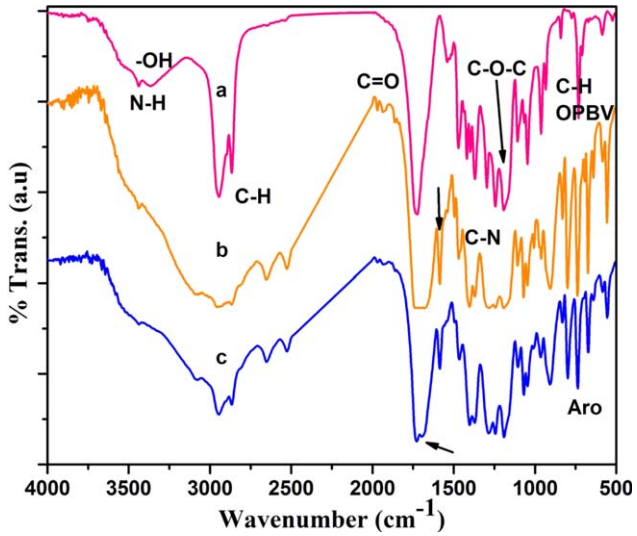

Figure 1. FTIR spectra of (a) L-glutathione-PCL, (b) PCL-L-glutathione-PTHF, (c) Ag-L-glutathione-PCL-PTHF nanocomposite system. [Color figure can be viewed in the online issue, which is available at wileyonlinelibrary.com.]

new peak at 1588 cm^{-1} corresponding to the tetrahydrofuronium ion[2] confirmed the ROP of THF. The ester C—O—C from PCL and ether C—O—C from PTHF appeared as a doublet peak at 1187 and 1282 cm^{-1} respectively. The aromatic (Aro) C—H bending can be seen at 662, 801 and 823 cm^{-1}. This is due to the ortho disubstituted phenyl ring of PAH. The appearance of aromatic C-H stretching, tetrahydrofuronium ion, ether C—O—C linkage and ortho disubstituted phenyl ring peaks confirmed the diblock copolymer formation in the presence of PAH as a comonomer. Figure 1(c) represents the FTIR spectrum of nano Ag end capped diblock copolymer. Here also the peaks corresponding to PCL and PTHF were noticed. Even then, some peaks were well isolated. The C—S (1398 cm^{-1}) and C—N (1367 cm^{-1}) stretching aliphatic C-O-C from ester linkage (1187 cm^{-1}), aromatic C—O—C linkage(1244 cm^{-1}) and aliphatic ether C—O—C linkage (1276 cm^{-1}) were clearly appeared. This confirmed the interaction among the Ag nanoparticle, PCL and PTHF segments. The Ag nanoparticle is formed due to the reduction activity of -SH group of L-glutathione and by the polyol methodology. The polyol methodology is a slower one whereas the reduction by thiol group is a faster one. The Ag nanoparticle is absorbed by the amino, thiol, ester and ether group of the L-glutathione, PCL and PTHF segments. There is no separate peak due to Ag nanoparticle. Thus, the FTIR spectrum confirmed the functional groups present in the polymer systems.

The chemical structures of homo and diblock copolymers were confirmed by NMR spectroscopy. The ^1H-NMR spectrum of L-glutathione end capped PCL is given in Supporting Information Figure S1. Supporting Information Figure S1(a) indicates the ^1H-NMR spectrum of L-glutathione end capped PCL. A sharp peak at 0 and 6.9 ppm are corresponding to internal standard TMS and $CDCl_3$ solvent. A peak at 3.9 and 2.2 ppm corresponding to —O—CH_2—, —CO_2—CH_2[2,41,43] protons. The remaining NMR signals are matched with the structure. Peaks

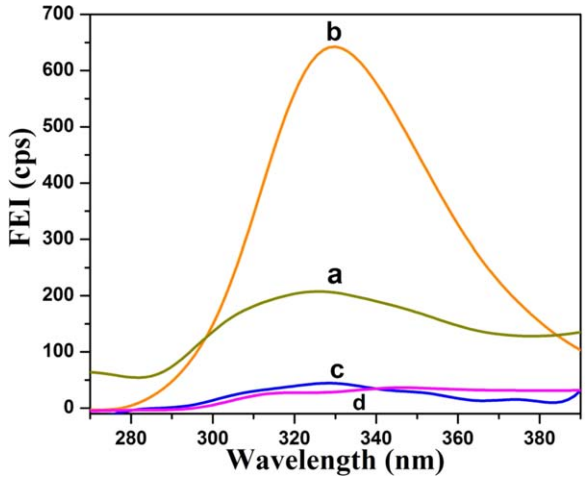

Figure 2. Fluorescence emission spectra of (a) L-glutathione, (b) L-glutathione-PCL, (c) PCL-L-glutathione-PTHF, (d) Ag-L-glutathione-PCL-PTHF nanocomposite system. [Color figure can be viewed in the online issue, which is available at wileyonlinelibrary.com.]

due to L-glutathione are not observed, which mean that it may not be solvated by $CDCl_3$ solvent. Supporting Information Figure S1(b) indicates the ^{13}C-NMR spectrum of L-glutathione end capped PCL. A carbon signal at 172 ppm is associated with the carbonyl carbon. A sharp peak at 74 ppm is due to the solvent. The peak at 62 ppm is due to $-OCH_2$ carbon signal. A $-CO_2-CH_2$ carbon signal appeared at 32 ppm and the remaining carbon signal are matched with the structure. Thus the NMR spectrum confirmed the chemical structure of L-glutathione end capped PCL. Supporting Information Figure S1(c) indicates the ^{1}H—NMR spectrum of diblock copolymer. Here also one can notice the above said peaks corresponding to the PCL segments. New peaks between 7.5 and 8.0 ppm confirms the formation of diblock copolymer. These proton signals are due to the aromatic protons of PAH, unfortunately peaks corresponding to PTHF segments are not observed. This indicates that the THF segments were not solvated by $CDCl_3$ solvent. Supporting Information Figure S1(d) confirms the ^{13}C—NMR spectrum of diblock copolymer. Appearance of new peaks between 129 and 135 ppm confirm the presence of aromatic carbons. Here also the carbon signals due to PTHF segments were not observed. Supporting Information Figure S1(e) and (f) indicates the ^{1}H and ^{13}C—NMR spectrum of nano Ag end capped diblock copolymer. There is no new peak corresponding to Ag nanoparticle. Hence, the NMR spectra confirmed the nano Ag end capped diblock copolymer.

The fluorescence emission spectrum of pristine L-glutathione is shown in Figure 2(a). An emission peak appeared at 329.6 nm. Figure 2(b) represents the emission peak of L-glutathione end capped PCL. Here also the same emission peak was observed at 329.6 nm but with high emission intensity. This confirmed that L-glutathione successfully initiated the ROP of CL. The increase in fluorescence emission intensity (FEI) is due to the [M/I] =100. The availability of more and more initiator (L-glutathione) is responsible for the high FEI value. Figure 2(c) indicates the fluorescence emission peak of diblock copolymer which produced a peak at 329.6 nm. The decrease in FEI value is due to the decrease in L-glutathione concentration. Here the intensity was found to be reduced when compared with the homo PCL. Figure 2(d) indicates the fluorescence emission spectrum of nano Ag end capped diblock copolymer. Here the emission peak shifted to 315.6 nm. The fluorescence emission spectrum of silver nanoparticles is characterized by the two peaks.[34] Emission spectra is not visible for nano Ag end capped diblock copolymer though it is dependent the concentration of L-glutathione. The blue shift in the peak is due to the incorporation of Ag nanoparticles which may quench the fluorescence emission phenomenon of L-glutathione. Due to this reason the emission peak was blue shifted with decrease in emission intensity. The fluorescence emission spectrum of L-glutathione was thoroughly studied by Lieberman and co-workers.[30] Due to the above said reasons, the present investigation yielded an entirely different result.

The ROP efficiency of L-glutathione is determined by GPC technique. Table I indicates the Mn, Mw and polydispersity (PD) values of polymer systems. The L-glutathione initiated ROP of CL is given in Figure 3(a). The M_w, M_n, and PD values are determined as 3415 g/mol, 2119 and 1.61 respectively. The PD value confirmed that L-glutathione is a suitable initiator for the ROP of CL. And also it confirmed the formation of homo PCL without any branching or cross linking. In the next step the L-glutathione end capped PCL is going to act as an initiator towards the ROP of THF in the presence of PAH as a comonomer. Figure 3(b) represents the GPC trace of diblock copolymer. Here also the Mw, Mn and PD values were determined as 3660 g/mol, 2056 and 1.78 respectively. The increase in the Mw confirmed the ROP of THF in the presence of PAH. Again the PD value informed that during the course of the ROP of THF there was no cross linking or branching. In the third step, diblock copolymer/Ag nanocomposite was prepared via polyol methodology. In this reaction Ag (+1) was reduced to Ag (0). After the preparation of diblock copolymer/Ag nanocomposites, again the Mw, Mn and PD values were determined (3868 g/mol, 2137 and 1.81 respectively, Figure 3(c). Thus the increase in molecular weight confirmed the formation of Ag nanoparticle. Due to the surface catalytic effect of Ag nanoparticle the Mw value of the diblock copolymer increased, via the Ag nanoparticle which is acting as a cross linking junction. As a result, the nanocomposite exhibited higher molecular weight than the homo and diblock copolymer. The nanoparticle formation is further confirmed by HRTEM. The present system produced somewhat lower molecular weight when compared with the literature.[43,44] This confirmed the less initiating efficiency of the L-glutathione towards the ROP of CL due to the structural entity. In the GPC traces, the unshaded area confirmed the GPC trace of original homopolymer (i.e.,) L-glutathione end caped PCL. The shaded area confirmed the increase in molecular weight of the polymer after the diblock copolymer formation and the incorporation of Ag nanoparticles. It means that the Ag nanoparticles are encapsulated by the diblock copolymer chains. Moreover, the change in molecular weight is very small.

Conjugation of hydrophobic PCL and hydrophilic PTHF through L-glutathione was characterized by HRTEM. Figure 4(a) indicates the HRTEM image of the diblock copolymer. The image shows

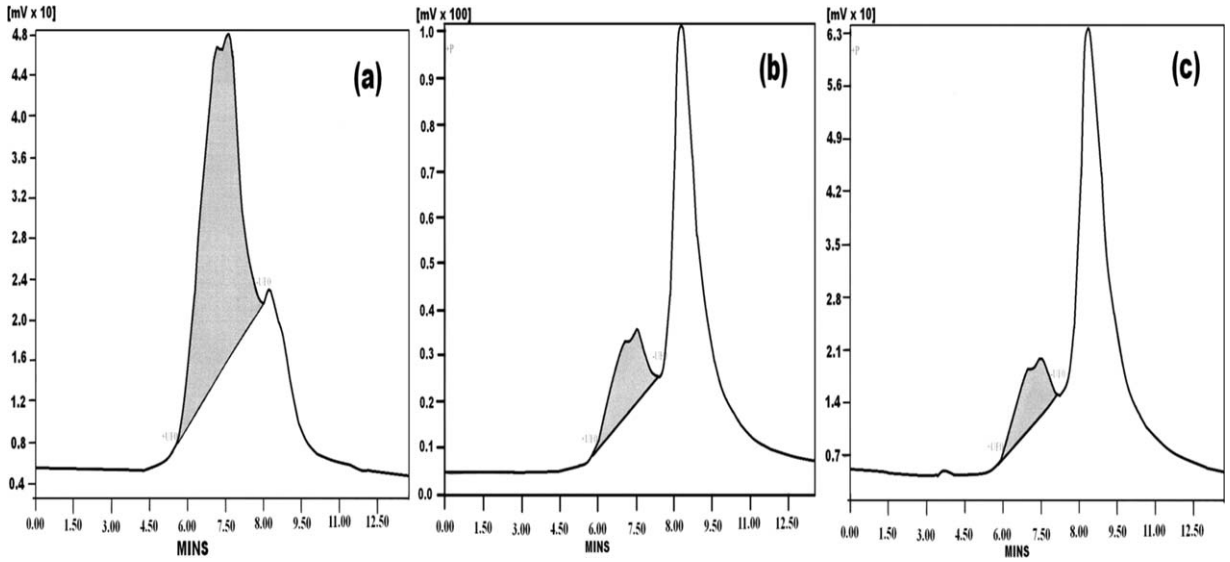

Figure 3. GPC traces of (a) L-glutathione-PCL, (b) PCL-L-glutathione-PTHF, (c) Ag-L-glutathione-PCL-PTHF nanocomposite system.

the distorted spheres and nanofiber like morphology due to the formation of polymer nanoparticles. Conjugation of both hydrophobic PCL and hydrophilic PTHF segments led to the formation of nanoparticles with different shape and size in accordance with the literature report.[2] The size of the distorted sphere was found to be < 20 nm whereas the length of the nanofiber was determined to be < 100 nm with the breadth of 3 nm. Figure 4(b) indicates the HRTEM image of nano Ag end capped diblock copolymer system. The image indicates the layered structure of Ag nanoparticle. The length of the layer was found to be 3–8 nm. Figure 4(c) indicates the HRTEM image of nano Ag end capped diblock copolymer system. The size of the silver nanoparticle was found to be 5 to 10 nm. Apart from these, nanomicelles are also seen with different shape like an octopus. Above all, the Ag nanoparticle is noticed without any agglomeration. The surface catalytic effect of Ag nanoparticle played a vital role in predicting the size and shape of polymer nanomicelles.

The surface morphology of L-glutathione end capped PCL is shown in Figure 5(a). Here one can see a nanofiber like morphology. The breadth of the fiber was determined as 110 nm whereas the length of the fiber varied between 1 to several μm. This indicates that the initiator itself can tune the surface morphology of PCL. Normally, the PCL exhibits the dried sky or broken stone like morphology.[44] In the present investigation, the surface morphology of PCL is completely altered by the initiator. Moreover, system of PCL in its fiber form is a time and money saving process. Above all, the PCL formation occurred by a bulk polymerization method which is an environmental green method. Figure 5(b) indicates the FESEM image of the diblock copolymer, again one can see the nanofiber structure with two distinct regions. The lower region is corresponding to the nanofiber formation of PCL whereas the upper region is due to the fiber formation of PTHF segments. In both regions the diameter of the fiber is around 100 nm, whereas the length of the fiber extends up to several μm. The nanofiber formation of hydrophobic PCL and hydrophilic PTHF is a suitable candidate for an effective drug delivery process. This is the novelty of the present investigation. Figure 5(c) indicates the FESEM image of nano Ag end capped diblock copolymer system. Again the

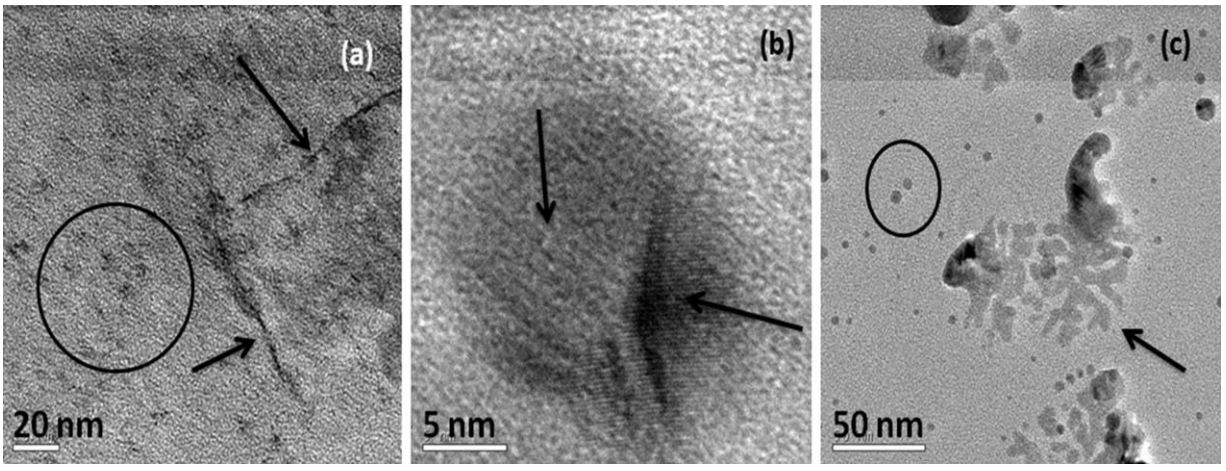

Figure 4. HRTEM image of (a) PCL-L-glutathione-PTHF, (b) Ag-L-glutathione-PCL-PTHF, (c) Ag-L-glutathione-PCL-PTHF nanocomposite system.

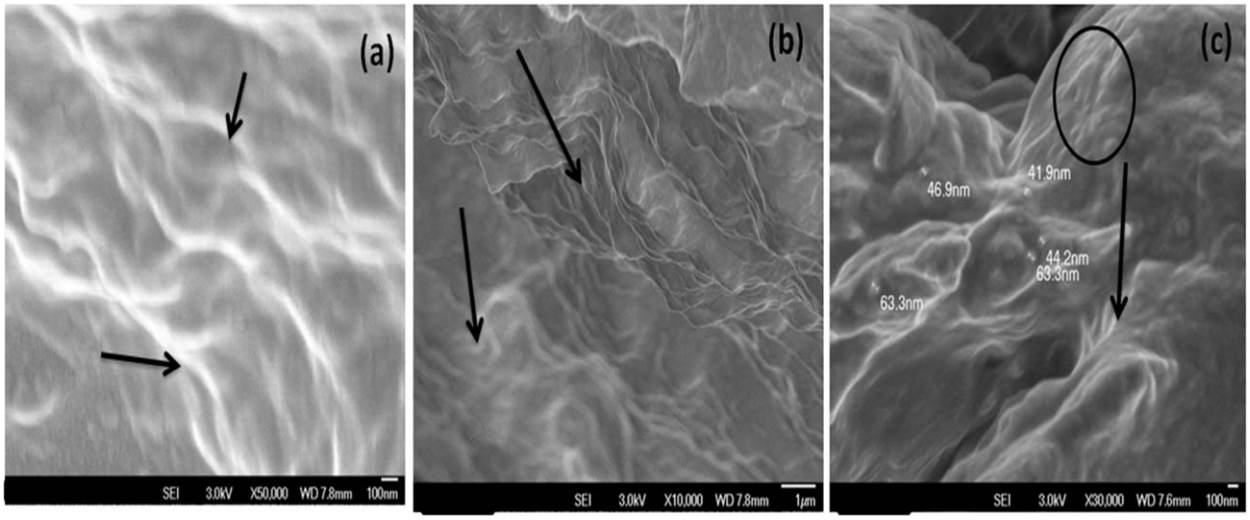

Figure 5. FESEM image of (a) L-glutathione-PCL, (b) PCL-L-glutathione-PTHF, (c) Ag-L-glutathione-PCL-PTHF nanocomposite system.

image showed a fiber like structure with uniform distribution of Ag nanoparticle. The size of the Ag nanoparticle varied between 30 and 65 nm that is in accordance with HRTEM report. The FESEM results concluded that PCL can be converted into nanofiber form by a simple ROP in the presence of L-glutathione initiator system. The EDAX spectrum of diblock copolymer nanocomposites is given in Figure 6. Here the peak corresponding to C, O, N, S and Ag were appeared. The percentage contents of the elements such as C (75.3%), O(13.4%), N(6.5%), S(3.3%) and Ag(1.56%) were determined and confirmed the formation of nano Ag end capped diblock copolymer system.

The DSC curve infers the thermal transition involved in the polymer systems. The DSC curve of L-glutathione initiated ROP of CL is given in Figure 7(a). The system exhibits an endothermic peak at 64.3 °C due to the melt transition (T_m) of PCL in accordance with Kannammal and co-workers report.[43] Figure 7(b) represents the T_m of the diblock copolymer that appeared at 63.17 °C, as compare to the T_m of homopolymer the copolymer exhibited the lowest temperature.[2] This is due to the presence of hydrophilic PTHF segment that absorbs moisture from the atmosphere and results reduction in the T_m of the copolymer.[2] Figure 7(c) represents the DSC curve of nano Ag end capped diblock copolymer. The T_m appeared at 64.3 °C which indicates that after the incorporation of Ag nanoparticles the hydrophobicity was increased and hence the T_m due to PCL was increased. Moreover, the Ag nanoparticle acts as a cross linking center as a result the molecular weight of the nano Ag end capped diblock copolymer system is slightly increased. The increase in molecular weight may induce the increase in T_m of the nano Ag end capped diblock copolymer. The shape of the peak was widening after the diblock copolymerization. This confirmed the inclusion of amorphous PTHF segments in the semi-crystalline PCL chains.

The thermal stability of polymer was confirmed by TGA. Figure 8(a) represents the TGA curve of L-glutathione end capped PCL. The curve exhibited a two step degradation process. The first major weight loss around 360 °C is ascribed to the degradation of PCL backbone.[44] The second minor weight loss around 450 °C is due to the degradation of L-glutathione. Figure 8(b) indicates the TGA curve of diblock copolymer. Here the curve

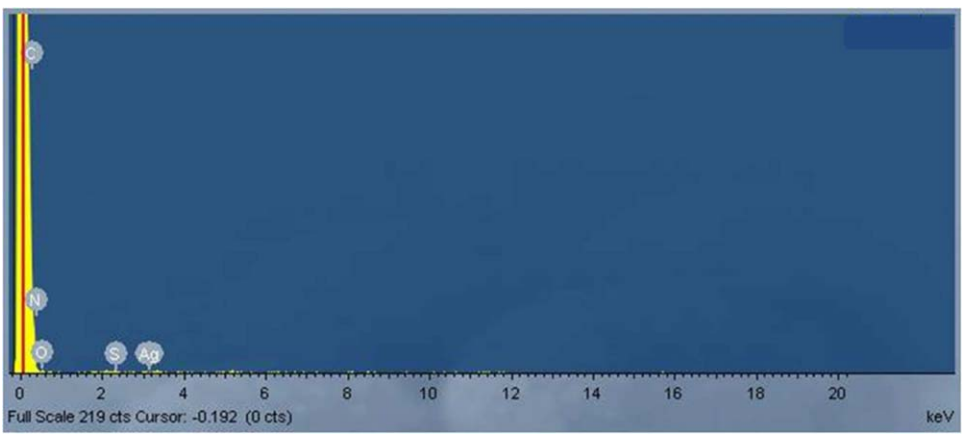

Figure 6. EDAX spectrum of Ag-L-glutathione-PCL-PTHF nanocomposite system. [Color figure can be viewed in the online issue, which is available at wileyonlinelibrary.com.]

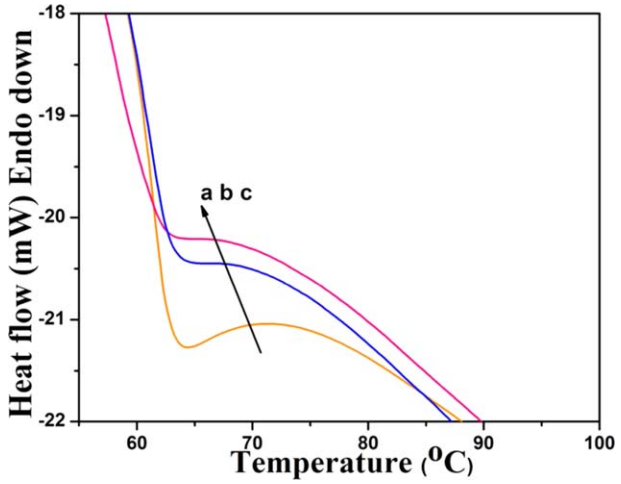

Figure 7. DSC curve of (a) L-glutathione-PCL, (b) PCL-L-glutathione-PTHF, (c) Ag-L-glutathione-PCL-PTHF nanocomposite system. [Color figure can be viewed in the online issue, which is available at wileyonlinelibrary.com.]

exhibited a three step degradation process. The first major weight loss around 250 °C is explained on the basis of degradation of hydrophilic PTHF segments.[2,41] The second major weight loss around 340 °C is due to degradation of PCL segments. The third minor weight loss around 500 °C is explained on the basis of degradation of L-glutathione. The diblock copolymer exhibited low thermal stability than the homo PCL due to the introduction of moisture absorbing PTHF segments. Figure 8(c) represents the TGA curve of nano Ag end capped diblock copolymer with four step degradation processes. The first major weight loss around 230 °C is due to the degradation of hydrophilic PTHF segments. The second weight loss around 315 °C is associated with the degradation of hydrophobic PCL segment.[44] The third minor weight loss around 385 °C is due to the degradation of PCL very nearer to the Ag nanoparticle (i.e,) the thiol group of L-glutathione interacted with $AgNO_3$ to form Ag-S bond. While heating to 400 °C the Ag-S bond undergoes degradation. The fourth minor weight loss around 450 °C is due to the degradation of L-glutathione. Above 550 °C the system exhibited 4.2% weight residue remained. This is due to the presence of Ag nanoparticle. In overall comparison, the nano Ag end capped diblock copolymer exhibited the lowest degradation temperature for PTHF and PCL degradation but above 550 °C the later system exhibited high % weight residue remained. In 2004, Lee and co-workers[45] studied about the thermal stability of Ag-oleate complex. Here the major weight loss step was appeared around 300 °C. When compared with the literature the present system yielded a good thermal stability.

The CD study confirms the change in the conformation of L-glutathione before and after making the amphiphilic diblock copolymer. Figure 9(a) indicates the CD spectrum of L-glutathione-PCL system. The CD spectrum exhibits two negative peaks at 214 and 227 nm. Appearance of these two peaks confirms the levorotatory nature of L-glutathione-PCL system. Figure 9(b) represents the CD spectrum of L-glutathione-PC L-PTHF system. In this case, first peak appeared at 216 nm whereas the second peak at 227 nm disappeared. Instead, a strong triplet peak was observed at 237, 241 and 243 nm. This indicates that even after amphiphilic diblock copolymer formation, the conformation of L-glutathione has not changed. The appearance of new peaks can be ascribed to the surface charges present on the PTHF segments (i.e,) formation of tetrahydrofuronium ion. Figure 9(c) represents the CD spectrum of Ag nanoparticle end capped amphiphilic diblock copolymer. Here one can see the above said peaks with more clearance. The first peak appeared

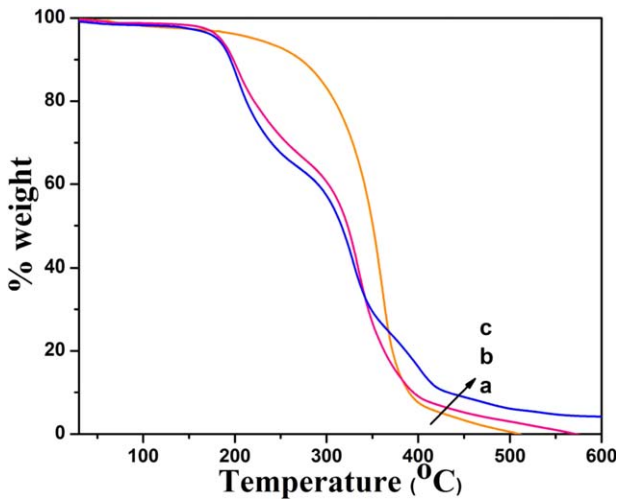

Figure 8. TGA curve of (a) L-glutathione-PCL, (b) PCL-L-glutathione-PTHF, (c) Ag-L-lutathione-PCL-PTHF nanocomposite system. [Color figure can be viewed in the online issue, which is available at wileyonlinelibrary.com.]

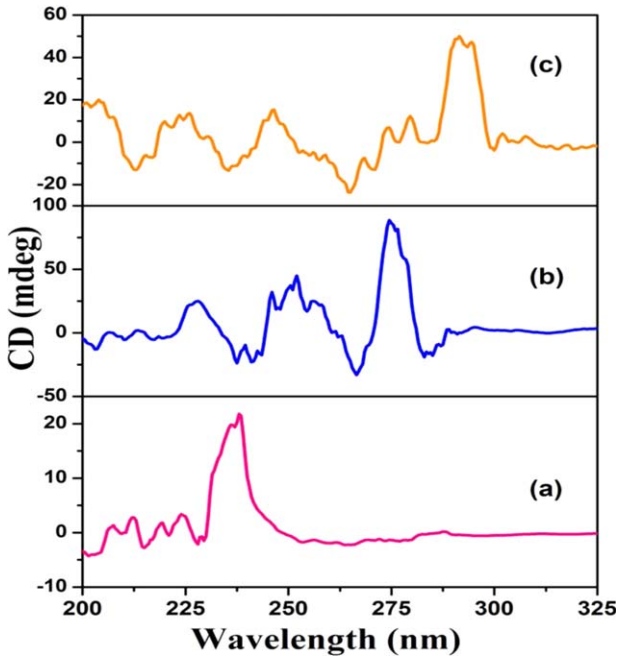

Figure 9. Circular dichroism spectrum of (a) L-glutathione-PCL, (b) PCL-L-glutathione-PTHF, (c) Ag-L-glutathione-PCL-PTHF nanocomposite system. [Color figure can be viewed in the online issue, which is available at wileyonlinelibrary.com.]

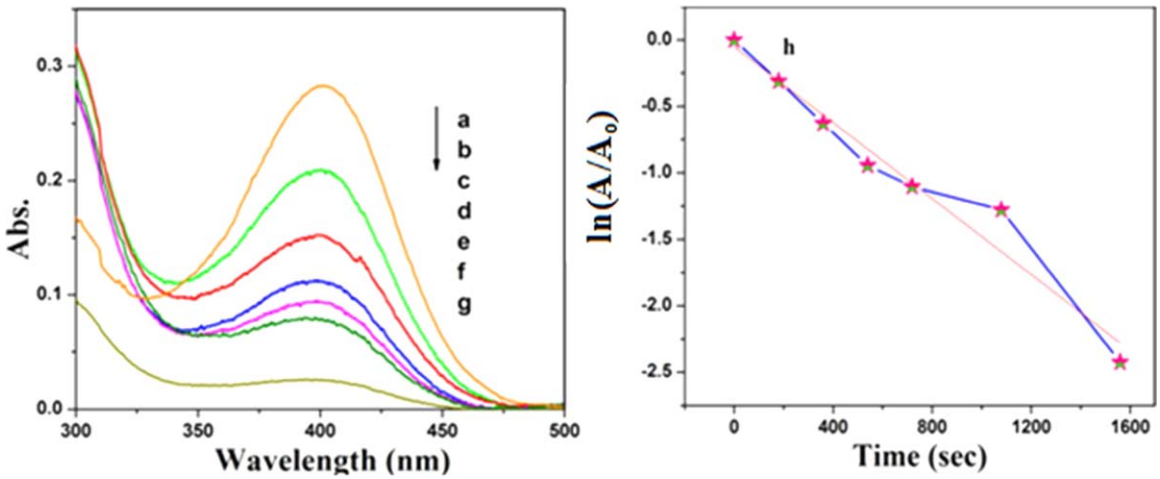

Figure 10. UV–visible spectrum of 4-NP taken at different time interval (a) 0 min, (b) 3 min, (c) 6 min, (d) 9 min, (e) 12 min, (f) 15 min, (g) 18 min, (h) plot of time vs. $\ln(A/A_o)$. [Color figure can be viewed in the online issue, which is available at wileyonlinelibrary.com.]

at 212 nm, whereas the second peak appeared at 235 nm as a multiplet peak. Again this confirms the existence of L conformation with the same charges. The CD study indicated that the conformation of L-glutathione has not altered even after three different chemical reactions. In the earlier communication, it is noted that the conformation of L-cysteine alters at each chemical reaction step.[41] But, the present system does not show any change in conformation during the chemical reactions even at higher temperature. The CD spectrum of L-glutathione is not included here because lot of report is available in the literature.[41]

The ultimate aim of the present investigation is the testing of polymer systems towards the splinting application. A material is suitable for splinting application when it has good tensile strength, particularly greater than that of the raw fabric, and % elongation. The advantage of the present investigation is increase of tensile strength with antimicrobial property. The raw fabric exhibited the tensile strength and % elongation values of 1846.8 kg/cm^2 and 38.45% respectively. The P1 coated fabric exhibited higher tensile strength (2764 kg/cm^2) value and lower % elongation (27.2%) value than the raw fabric. The increase in tensile strength value is explained on the basis of coating of hydrophobic PCL. The hydrophobic nature of PCL accelerates the interaction between the raw fabric and PCL segments. The presence of good interaction between them the tensile strength value increases greatly. The % elongation value is reduced as a result of increase of rigidity. The P2 coated fabric exhibited lower tensile strength (1500 kg/cm^2) value when compared with the P1 coated fabric and raw fabric. The PTHF segments led to the moisture gaining nature.[2,41] As a result of moisture absorption the tensile strength value reduced drastically. At the same time the % elongation (55.3%) value was 1.5 times greater than that of raw fabric and two times greater than the P1 coated fabric. Again the moisture adsorption gives the explanation for the increase in % elongation. The P3 coated fabric exhibited higher tensile strength (3371 kg/cm^2) value than the raw fabric, P1 and P2 coated fabrics. This can be explained as follows. The abnormal increase in tensile strength value is ascribed to the Ag nanoparticle. Sometimes the Ag nanoparticle may act as nanofiller and hence the voids between the polymers can be filled by the Ag nanoparticles. As a result, the tensile strength value was increased greatly. Moreover, the P3 coated fabric system exhibited hydrophilic nature, unfortunately the % elongation (23.8%) value depressed due to the increase in rigidity. The tensile testing report confirmed that our polymer systems are suitable for low temperature splinting application. Supporting Information Figure S2 indicates the picture of raw fabric, P1, P2 and P3 coated fabric towards low temperature splinting application. Both PCL and PTHF have low melting point and are suitable for low temperature splinting application. This can be confirmed by referring Supporting Information Figure S2. Supporting Information Figure S2(a) indicates that the raw fabric is not suitable for desired shape, because after cooling the shape of the cloth was collapsed. Supporting Information Figure S2(b–d) were maintained the shape even after cooling. These pictures supported that our polymer systems suitable for low temperature splinting application. The presence of silver nanoparticle with antimicrobial property is confirmed by the brown coloration [Supporting Information Figure S2(d)].

The wound healing activity of the fabric before and after coating with polymer was tested by the adsorption of water and chloroform. The raw fabric exhibited the water and chloroform absorption values of 5.37 g/5 min and 4.86 g/5 min respectively. After coating with P1 the water absorption was reduced due to the hydrophobic nature of polymer system whereas the chloroform absorption was improved due to the dissolution of PCL in chloroform. The fabric on coating with P2 exhibits the high water absorption value (5.66 g/5 min) and moderate chloroform absorption value. This confirmed the hydrophilic nature of P2. The P3 coated fabric exhibited the moderate water absorption value and higher chloroform absorption value. Again this confirms the hydrophobic nature. In general, absorption study inferred that our polymer system is suitable for the self-cleaning and wound healing application. In present investigation the

wound healing activity is studied in terms of water and chloroform absorption. The combination of both hydrophobic and hydrophilic segments is more helpful to absorb the waste water and puss coming out from the wound. The Ag nanoparticle offers the antimicrobial activity which is confirmed in the earlier publication.[34,41] Hence, the present polymer systems are suitable for low temperature splinting and wound healing application.

Nanomaterials found wide applications in various science and engineering fields.[46,47] Generally, the nano materials are used in catalysis field as a catalyst. In the present investigation the nanosized Ag is chemically attached with the thiol group of L-glutathione and encapsulated by the -OH group of PCL or PTHF. It means some of the Ag nanoparticles are chemically attached with amphiphilic copolymer chain whereas the remaining is simply dispersed on the polymer matrix. Here, the catalytic effect of Ag nanoparticles towards the reduction of NP was taken as a standard model. The reaction was monitored by UV-visible spectrophotometer with 3 min interval of time. It was found that while increasing the reaction time, the absorbance at 400 nm reduced slowly. This is due to the conversion of NP into aminophenol. Figure 10(a–g) indicates the same. From the absorbance value the apparent rate constant value was determined by plotting $\ln(A_t/A_0)$ where A_0 and A_t is the absorbance of NP at time 0 and time t. In the methodology part it is mentioned as $\ln(A/A_0)$. It is very convenient to note that the absorbance measured at any time can be easily understood. Hence, better it should be (A_t/A_0). Figure 10(h) indicates the above said plot with the slope value of 1.4×10^{-3} sec^{-1}. This proved that the Ag nanoparticle has surface catalytic effect and acted as a typical catalyst towards the reduction reaction. The important point noted here is, in the absence of Ag nanoparticle the reduction of NP was found to be nil. When compared to literature value,[48] the present system yielded the apparent rate constant value of $3.22 \times 10^{-3} sec^{-1}$. Hence, the present nano Ag end capped diblock copolymer system proved the surface catalytic effect of Ag nanoparticle.

CONCLUSIONS

The present investigation summarizes the niche points as conclusion. The appearance of doublet C═O stretching around 1715 cm^{-1} in the FTIR spectrum confirmed the diblock copolymerization between CL and THF monomers. Due to the hydrophilic nature, the diblock copolymer exhibited lower thermal degradation temperature (T_d). The diblock copolymer formation was confirmed by GPC analysis. The —O—CH_2— signal of PCL appeared around 4.2 ppm in the ^{1}H-NMR spectroscopy. The GPC result declared that while moving from step 1 to step 3, both the M_w and M_n increased gradually. The homo PCL exhibited the dried sky like morphology whereas the diblock copolymer exhibited the fibrous morphology and the nano Ag end capped diblock copolymer exhibited the original surface morphology with the size of approximately 50 nm. The HRTEM images represented that the diblock copolymer exhibited the nanorod like morphology with the layered structure. The length of nanorod was determined as 10–15 nm. The % content of Ag nanoparticle was confirmed by EDAX. The fluorescence property of L-glutathione was confirmed by fluorescence emission spectroscopy, appeared around 330 nm. The CD study indicated the absence of change in conformation even after homo and diblock copolymer formation. The decrease in tensile strength and increase in % elongation of the diblock copolymer confirmed the amphiphilic copolymer formation. Water and chloroform absorption study indicated that the amphiphilic copolymer consists of both hydrophilic and hydrophobic segments and is a suitable candidate for the low temperature splinting application. The catalytic reduction study indicated the apparent rate constant value as 3.22×10^{-3} sec^{-1} and extended the application of amphiphilic diblock copolymer nanocomposite as a catalyst towards the reduction of NP. The present investigation recommended that the Ag nanoparticle end capped diblock copolymer is a suitable candidate for the low temperature splinting application as well as a catalyst for the reduction of NP.

ACKNOWLEDGMENTS

Dr.N. Sundararajan, Associate Professor, Department of English is gratefully acknowledged for his valuable help during this manuscript preparation work.

REFERENCES

1. Salgado, C. L.; Sanchez, E. M.; Zavaqlia, C. A.; Granja, P. L. *Tissue Eng. Part A* **2012**, *18*, 137.
2. Kailash, S.; Meenarathi, B.; Palanikumar, S.; Anbarasan, R. *Int. J. Polym. Mater. Polym. Biomater.* **2015**, *64*, 620.
3. Manikandan, B.; Meenarathi, B.; Anbarasan, R. *Int. J. Appl. Eng. Res.* **2015**, *10*, 695.
4. Meenarathi, B.; Priyadarshini, B.; Muthuprasannavathana, J.; Anbarasan, R. *Int. J. Sci. Res. Eng. Tech.* **2014**, *1*, 9.
5. Meenarathi, B.; Anbarasan, R. *Int. J. Sci. Res. Eng. Tech.* **2014**, *1*, 15.
6. Sowkath, A.; Ahmad, M.; Anbarasan, R. *Int. J. Emerg. Tech. Eng.* **2014**, 15.
7. Savaskan, S.; Hazer, B. *Angew. Chem.* **1996**, *239*, 13.
8. Wu, B.; Lenz, R. W.; Hazer, B. *Macromolecules* **1999**, *32*, 6856.
9. Seyednejad, H.; Gawlitta, D.; Kuiper, R. V.; Bruin, A.; Vermonden, T.; Dhert, W. J. A.; Hennink, W. E. *Biomater* **2012**, *33*, 4309.
10. You, J. H.; Choi, S. W.; Kim, J. H.; Kwak, Y. T. *Macromol. Res.* **2008**, *16*, 609.
11. Zhao, Y.; Hu, T.; Lv, Z.; Wang, S.; Wu, C. *J. Polym. Sci. B Polym. Phys.* **1999**, *37*, 3288.
12. Cuong, N. V.; Hsieh, M. F.; Chen, Y. T.; Liau, I. *J. Appl. Polym. Sci.* **2010**, *117*, 3694.
13. Hazer, B. *Eur. Polym. J.* **1990**, *26*, 1167.
14. Hazer, B. *J. Polym. Sci. Part A Polym. Chem.* **1987**, *25*, 3349.
15. Hazer, B.; Cakmak, I.; Denizligil, S.; Yagci, Y. *Die Angew. Makromol. Chem.* **1992**, *195*, 121.
16. Hazer, B.; Baysal, B. M.; Koseoglu, A. G.; Besirli, N.; Taskin, E. *J. Polym. Environ.* **2012**, *20*, 477.

17. Bates, F. S.; Fredrickson, G. H. *Ann. Rev. Phys. Chem.* **1990**, *41*, 525.
18. Kamigaito, M.; Ando, T.; Sawamoto, M. *Chem. Rev.* **2001**, *101*, 3689.
19. Guo, A.; Yang, F.; Yu, R.; Wu, Y. *Chin. J. Polym. Sci.* **2015**, *33*, 23.
20. Bouchama, A.; Ferrahi, M. I.; Belbachir, M. J. *Chem. Sci.* **2012**, CSJ40.
21. Sari, F.; Ferrahi, M. I.; Belbachir, M. *Bull. Chem. React. Eng. Catal.* **2012**, *7*, 165.
22. Misir, M.; Ozturk, T.; Emirik, M.; Yilmaz, S. S. *J. Polym. Sci. Part A: Polym. Chem.* **2010**, *48*, 2896.
23. Filimoshkin, A. G.; Kuchevskaya, A. S.; Berezina, E. M.; Ogorodnikov, V. D. *Exp. Polym. Lett.* **2009**, *3*, 13.
24. Fan, W. W.; Fan, X. D.; Tian, W.; Liao, X. Q.; Zhang, W. B.; Mu, C. G.; Kong, J. *Exp. Polym. Lett.* **2013**, *7*, 416.
25. Reddy, T. S.; Jayakumar, K. K.; Nair, J. K.; Satpute, R. S.; Mukundan, T. *Def. Sci. J.* **2006**, *56*, 399.
26. Hovetborn, T.; Holscher, M.; Keul, H.; Hocker, H. *Rev. Roum. Chim.* **2006**, *51*, 781.
27. Ferrahi, M. I.; Belbachir, M. *Int. J. Mol. Sci.* **2003**, *4*, 312.
28. Hepuzer, Y.; Serhatli, I. E.; Yagci, Y. *Eur. Polym. J.* **1998**, *34*, 631.
29. Hicks, L. M.; Cahoon, R. E.; Bonner, E. R.; Rivard, R. S.; Sheffield, J.; Jez, J. M. *Plant Cell Online* **2007**, *19*, 2653.
30. Lieberman, I.; Shemer, G.; Fried, T.; Kosower, E. M.; Markovich, G. *Angew. Chim. Int. Ed.* **2008**, *47*, 4855.
31. Li, T.; Park, H. G.; Lee, H. S.; Choi, S. H. *Nanotech* **2004**, *15*, S660.
32. Carlberg, I.; Sjodin, T.; Mannervik, B. *Eur. J. Biochem.* **1980**, *112*, 487.
33. Hakimi, M.; Aliabadi, T. S. *World Appl. Prog.* **2012**, *2*, 431.
34. Ramkumar, P.; Kamaraja, D.; Vinothraj, R.; Anbarasan, R. *Adv. Appl. Sci. Res.* **2015**, *6*, 7.
35. Hsu, K. C.; Chen, D. H. *Nanoscale Res. Lett.* **2014**, *9*, 484.
36. Leelavathi, A.; BhaskaraRao, T. U.; Pradeep, T. *Nanoscale Res. Lett.* **2011**, *6*, 1.
37. Zheng, Y.; Zhu, Y.; Tian, G.; Wang, A. *Int. J. Biol. Macromol.* **2015**, *73*, 39.
38. Bingwa, N.; Meijboom, R. *J. Mol. Cat. A. Chem.* **2015**, *396*, 1.
39. Ravula, S.; Essner, J. B.; LA, W. A.; Parade, L. P.; Kargupta, R.; Hull, G. J.; Sengupta, S.; Baker, G. A. *Nanoscale* **2015**, *7*, 86.
40. Meenarathi, B.; Kannammal, L.; Palanikumar, S.; Anbarasan, R. *Mater. Res. Exp.* **2014**, *1*, 1.
41. Jeyapriya, M.; Meenarathi, B.; Kannammal, L.; Anbarasan, R. *Chin. J. Polym. Sci.* **2015**, *10*, 1.
42. Kalyaci, O.; Comert, F. B.; Hazer, B.; Atlay, T.; Cavicchi, K. A.; Cakmak, M. *Polym. Bull.* **2010**, *65*, 215.
43. Kannammal, L.; Meenarathi, B.; Palanikumar, P.; Anbarasan, R. *J. Phys. D Appl. Phys.* **2014**, *47*, 135109.
44. Meenarathi, B.; Kannammal, L.; Palanikumar, S.; Anbarasan, R. *Spectrochim. Acta Part A* **2014**, *135*, 93.
45. Lee, D. K.; Kang, Y. S. *ETRI J* **2004**, *26*, 252.
46. Parveen, M. F.; Umapathy, S.; Dhanalakshmi, V.; Anbarasan, R. *Nano* **2009**, 4 147.
47. Palanikumar, S.; Siva, P.; Meenarathi, B.; Kannammal, L.; Anbarasan, R. *Intern. J. Biol. Macromol.* **2014**, *67*, 91.
48. Wunder, S.; Polzer, F.; Lu, Y.; Mei, Y.; Ballauf, M. *J. Phys. Chem. C* **2010**, *114*, 8814.